

On the thinning variations in hydrostatic forming of sheet metal

N.T. Thu¹, N.D. Trung¹¹ School of Mechanical Engineering, Hanoi University of Sciences and Technology, Hanoi, Vietnam

Phone: +84976512385

ABSTRACT – In sheet metal forming, thinning phenomenon is one of the most concerned topics to ameliorate the final quality of the manufactured parts. The thinning variations depend on many input parameters, such as technological parameters, geometric shape of die, workpiece's materials, and forming methods. Hydrostatic forming technology is particularly suitable for forming thin-shell products with complex shapes. However, due to the forming characteristics, the thinning variations in this technology are much more intense than in other forming methods. Therefore, in this paper, an empirical study is developed to determine the thinning variations in hydrostatic forming for cylindrical cup. Measurement of thickness at various locations of deformed products are conducted to investigate the thickness distribution and determine the dependence of the largest thinning ratio on the input parameters (including the blank holder pressure, the relative depth of the die and the relative thickness of the workpiece). The results are expressed in charts and equation which allow determining the effect of each input parameter on the largest thinning ratio.

ARTICLE HISTORY

Received: 21st Sept 2019Revised: 29th Sept 2020Accepted: 18th Nov 2020

KEYWORDS

*Hydrostatic forming;
largest thinning ratio;
blank holder pressure;
forming pressure;
sheet metal forming*

INTRODUCTION

Nowadays, sheet metal products play an important role in most sectors such as automotive, aviation, and civil engineering. Therefore, different methods of sheet metal forming have been researched and developed. This tendency has made a big motivation for studies on sheet technology to be done with considerable achievements [1-6]. In sheet metal forming process, thinning variations occur in most areas of the products and considerably affect the product quality, especially in drawing operation [2]. The thinning variations have been investigated and evaluated through typical parameters, including the largest thinning ratio of the product and thickness distribution [7, 8].

The largest thinning ratio is a ratio between the biggest thinning variation (ie, the difference of the initial thickness of workpiece and the minimum thickness of the product) and the initial thickness of workpiece. The ratio allows evaluating the product quality in the process. If the ratio is too high, there might be either visible cracks or microscopic cracks which reduce the strength of the product. In the thin-shell industry, this indicator is important to determine if a product is of good quality or not. Thickness distribution is a change in thickness at different locations on the product from the original workpiece thickness. In drawing operation for sheet metal, some regions on the product may be thickened, some may remain intact, while others may become thinner. Due to the characteristics of the forming process, the thickness distribution in hydrostatic forming differs from that of conventional forming.

Hydrostatic forming technology is one of the most emerging technologies that can be applied into manufacturing a lot of products in automobile and aerospace industries [9-11]. In this technology, the product is shaped in accordance with the die profile by a high liquid pressure source as shown in Figure 1. Hydrostatic forming for sheet metal has many advantages such as improving the ability to shape complex parts, increasing surface quality, and especially suitable for shaping lightweight and thin sheet materials [12-14]. Because of its superiority, there have been many studies on this technology over the years with different aspects of materials, temperatures, and die structures [15-20]. In hydrostatic forming process, the workpiece is remarkably thinned because of bulging phase under the action of a high-pressure liquid. Modi and Kumar [21] in the AA5182 material study showed that when the variable closing force was applied, the square cup product was more uniform in thickness and less thinned after forming than in case of constant closing force. Feyissa et al. [22] also presented that maximum percentage thinning reduced with the decrease in coefficient of friction from nearly 20% at ($\mu=0.25$) to 6% at ($\mu=0.04$) when studying the drawability of cryo-rolled AA5083 alloy sheets by hydrostatic forming. Zhang et al. [23] presented the causes of this thinning and indicated stress in each region. In addition, there are some studies to reduce thinning in the deformation stages [3, 24] especially in the period of free bulging, by using hard or soft opposite pressure. It can be seen that the thinning phenomenon has been of interest to many researchers in various aspects. However, the thickness distribution on hydrostatic formed products and the largest thinning ratio have not been specifically mentioned.

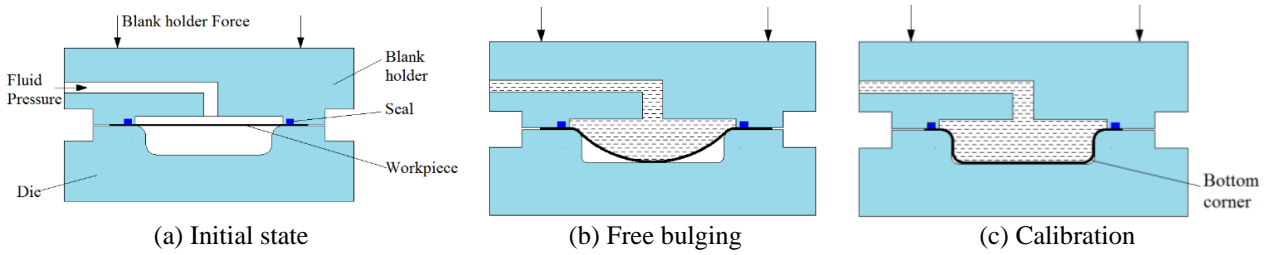


Figure 1. Diagram of hydrostatic forming

In this paper, an empirical study on hydrostatic forming technology for cylindrical cups is presented. The final products are measured in many positions to build a thickness distribution chart and determine the largest thinning ratio of each product. The measurement results of the largest thinning ratio are used to establish mathematical model showing the relationship between the largest thinning ratio and the input parameters including the blank holder pressure, the relative depth of die and the relative thickness of workpiece. The mathematical model has been obtained for certain conditions of the process execution.

METHODS AND MATERIALS

The research object is cylindrical product made of DC04 steel with initial thicknesses s_0 of 0.8 mm, 1.0 mm, 1.2 mm. It is formed in accordance with the die cavity as shown in Figure 2. The diameter of die d is 70 mm. Properties of DC04 steel are given in Table 1.

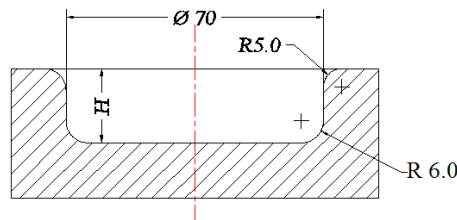


Figure 2. Geometric details of the cylindrical-shaped die

In this research, the depth of the die H is varied with three levels including 16.0 mm, 18.0 mm and 20.0 mm.

Table 1. Properties of material DC04

Yield stress (MPa)	Tensile strength (MPa)	Equivalent label
210~280	314~412	Russia-GOST 08kp Japan-JIS SPCE

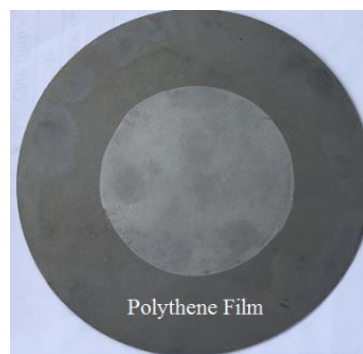


Figure 3. Workpiece covered with polythene on the outer flange

The diameter of workpiece D_0 is 110 mm and the workpiece is covered with a polythene film as shown in Figure 3. With the plastic film, the coefficient of friction is kept more stable in all experiments. The workpiece can slide easily on

the die surface and be pulled smoothly into the die cavity. Therefore, it can be assumed that the effect of friction in experiments is the same.

The relative depth of die H^* is calculated according to Eq. (1):

$$H^* = \frac{H}{d} * 100 \tag{1}$$

The relative thickness of workpiece S^* is calculated according to Eq. (2):

$$S^* = \frac{S_0}{D_0} * 100 \tag{2}$$

Research range of the blank holder pressure Q^* is of (80-115) bar. In order to solve the aims of the research, input variables and their value survey area are collected and given in Table 2.

Table 2. Input variables and research values

Independent variables	Coded variables	Research value
Q^*	x_1	80 ~ 115 (bar)
H^*	x_2	23.0, 26.0, 29.0 (%)
S^*	x_3	0.73, 0.91, 1.09 (%)

The experiment system consists of 4 modules as shown in Figure 4 including hydraulic 125-ton press, CP700 high-pressure pump, die system and measurement system.

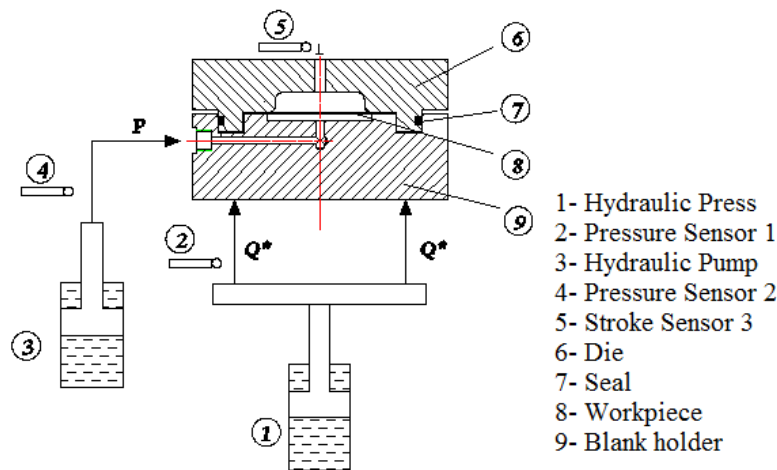


Figure 4. Schematic diagram of hydrostatic forming experiment system

Schematic diagram of forming a product by the hydrostatic forming method is presented in Figure 4. The workpiece is clamped between the hydrostatic die and the blank holder. High-pressure liquid is pumped into the groove gradually to form the product. The product is shaped according to the die shape. The changes in the pressure in the pump and the hydraulic press and the formation depth are recorded and monitored on the computer screen. Measuring microscope Mitutoyo MF is used to take photos of thickness of the product at 9 points as shown in Figure 5.

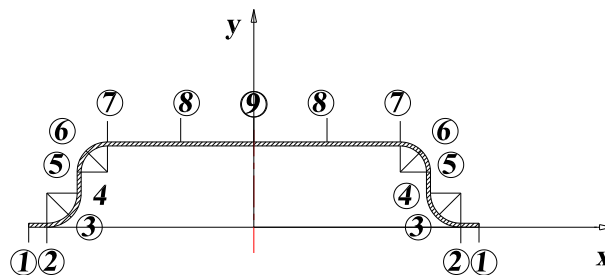


Figure 5. Measuring points on the product

RESULTS AND DISCUSSION

Evaluation the Thickness Distribution

In order to investigate the thickness distribution of products, the thickness deformation ratio γ is considered and determined by Eq.(3). The selected product for examination has the dimensions and the technological parameters as shown in Table 3.

$$\gamma = \frac{s_0 - s_i}{s_0} * 100 \tag{3}$$

Where s_i is the thickness value at each measuring position on the product (mm);

Table 3. Geometric parameters and technological parameters of the investigation case

Input parameters	Survey value
The thickness of workpiece, s_0 , mm	0.8
The depth of die, H, mm	16.0
The blank holder pressure, Q^* , bar	95.0, 100.0, 110.0, 115.0

The values of thickness at 9 measuring positions are converted into thickness deformation ratios according to the Eq. (3) and are collected in Table 4.

Table 4. Values of thickness deformation ratio (%)

Blank holder pressure (bar)	Value of each measuring point (%)								
	1	2	3	4	5	6	7	8	9
115	-2.87	-1.65	3.76	8.81	13.75	15.31	15.76	13.73	13.74
110	-4.44	-3.68	-2.87	4.09	8.16	10.61	10.83	9.69	8.70
105	-7.75	-6.37	-4.64	1.41	6.69	7.51	5.60	4.38	5.25
100	-7.86	-7.12	-4.85	1.08	5.81	7.36	8.34	4.85	6.34
95	-9.91	-7.60	-5.04	-0.60	4.46	7.69	8.14	4.48	5.68

Based on the results in Table 4, the thickness distribution charts are shown in Figure 6.

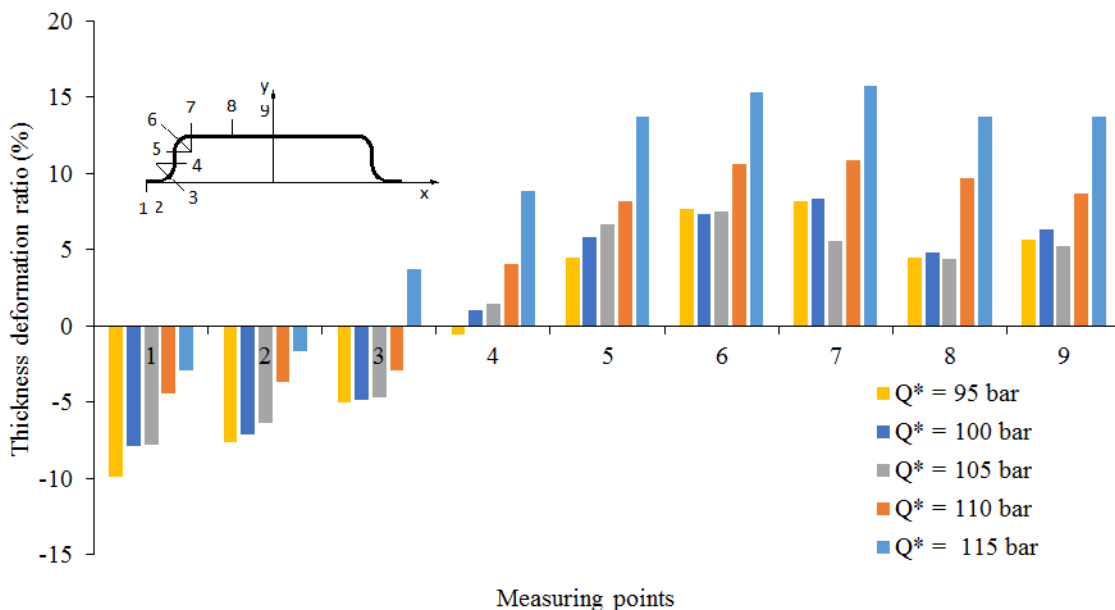


Figure 6. The thickness deformation ratio at measurement sites

The charts in the Figure 6 show the ratio of deformation at 9 measurement locations of the products at different blank holder pressure values. There are two main deformed regions on the product, including the thickening area (negative values) at part or all of the flange and the thinning area (positive values) at the body and bottom.

The charts in Figure 6 also show the change of thickening and thinning regions through different cases of blank holder pressure (95 bar, 100 bar, 105 bar, 110 bar and 115 bar). When the blank holder pressure is higher, the thinning region enlarges while the thickening region narrows. For each product, the flange or part of it is thickened (points 1, 2, 3, 4 under 95 bar of Q*; points 1, 2, 3 under (100~110) bar of Q*; points 1, 2 under 115 bar of Q*). This effect indicates that, in the flange region, the stress and deformation state of the product still obey the theory of metal plastic deformation for the conventional drawing process.

The product then starts to thin somewhere on the wall or the flange (point 3 under 115 bar of Q*, point 4 under (100-110) bar of Q* and point 5 under 95 bar of Q*). In all the measurement results, most values of thickness deformation ratio at three points (5, 6, 7) are higher than those of the remaining points. It means that the maximum thinning ratio occurs at a point on the rounded corner between the wall and the bottom. This can be explained by the friction between the workpiece and the die when forming. When the workpiece is exposed to the die, friction at the bottom and the wall of the die will prevent the workpiece from filling the corner radius. Therefore, the material is more prone to thinning and the product is more easily cracked in this area.

The graphs also show that thickness deformation ratio at point (8, 9) is less than at point (5, 6, 7). In hydrostatic forming technology, the material will contact the die's bottom under the effect of forming liquid pressure. Friction between the workpiece and the die's bottom prevents the movement of materials, so the workpiece in this area is less thinned. Through this study, it can be inferred that deformation on the flange of the product in hydrostatic forming technology is similar to the conventional drawing while deformation at the product body is different. The bottom radius of the product is the most thinned area due to the friction effect between the die and the workpiece. The investigation results propose that hard opposing pressure (here the bottom of the die) be also a good choice for reducing the thickness deformation ratio and improving the quality of product.

Building Mathematical Models of the Largest Thinning Ratio γ_{max}

Determination the largest thinning ratio

In this research, the orthogonal second order design specifies the number of experiments as shown in Eq. (4) [25]:

$$N=2^{k-p} + 2.k + n_0 = n_k + n_a + n_0 = 2^3 + 2.3 + 3 = 17 \tag{4}$$

In which, N is the total number of experiments, n_0 is the number of repetition in plan central, n_k is the number of change of variables, n_a is the number of symmetrically positioned points at plan central;

Coded values of physical quantities are obtained using following Eq. (5):

$$x_1 = \frac{Q^* - 97.5}{17.5}; \quad x_2 = \frac{H^* - 26}{3}; \quad x_3 = \frac{S^* - 0.91}{0.18} \tag{5}$$

Experimental array is established according to Table 5.

Table 5. Experimental array

Input variables of the process				Coded values										Vector output Y_i
Physical values														
No.	Q*	H*	S*	x_0	x_1	x_2	x_3	x_{12}	x_{13}	x_{23}	x'_1	x'_2	x'_3	
1	80.0	23	0.73	1	-1	-1	-1	1	1	1	0.27	0.27	0.27	Y_1
2	115.0	23	0.73	1	1	-1	-1	-1	-1	1	0.27	0.27	0.27	Y_2
3	80.0	29	0.73	1	-1	1	-1	-1	1	-1	0.27	0.27	0.27	Y_3
4	115.0	29	0.73	1	1	1	-1	1	-1	-1	0.27	0.27	0.27	Y_4
5	80.0	23	1.09	1	-1	-1	1	1	-1	-1	0.27	0.27	0.27	Y_5
6	115.0	23	1.09	1	1	-1	1	-1	1	-1	0.27	0.27	0.27	Y_6
7	80.0	29	1.09	1	-1	1	1	-1	-1	1	0.27	0.27	0.27	Y_7

Table 5. Experimental array (cont.)

Input variables of the process				Coded values										Vector output Y_i
Physical values														
No.	Q*	H*	S*	x ₀	x ₁	x ₂	x ₃	x ₁₂	x ₁₃	x ₂₃	x' ₁	x' ₂	x' ₃	
8	115	29	1.09	1	1	1	1	1	1	1	0.27	0.27	0.27	Y ₈
9	97.5	26	0.91	1	0	0	0	0	0	0	-0.73	-0.73	-0.73	Y ₉
10	97.5	26	0.91	1	0	0	0	0	0	0	-0.73	-0.73	-0.73	Y ₁₀
11	97.5	26	0.91	1	0	0	0	0	0	0	-0.73	-0.73	-0.73	Y ₁₁
12	118.8	26	0.91	1	1.215	0	0	0	0	0	0.75	-0.73	-0.73	Y ₁₂
13	76.2	26	0.91	1	-1.22	0	0	0	0	0	0.75	-0.73	-0.73	Y ₁₃
14	97.5	29.6	0.91	1	0	1.22	0	0	0	0	-0.73	0.75	-0.73	Y ₁₄
15	97.5	22.4	0.91	1	0	-1.2	1.0	0	0	0	-0.73	0.75	-0.73	Y ₁₅
16	97.5	26	1.13	1	0	0	1.215	0	0	0	-0.73	-0.73	0.75	Y ₁₆
17	97.5	26	0.69	1	0	0	-1.22	0	0	0	-0.73	-0.73	0.75	Y ₁₇

In order to determine the largest thinning ratio, each product is measured at 9 points as shown in Figure 5 and finds the point at which the thinnest thickness. The largest thinning ratio γ_{max} is determined by Eq. (6)

$$\gamma_{max} = \frac{s_0 - s_{min}}{s_0} * 100 \tag{6}$$

Where s_{min} is the minimum value of the product thickness (mm)
 Experimental results of the largest thinning ratio are collected in Table 6.

Table 6. Experiment results

N ₀	1	2	3	4	5	6	7	8	9	10	11	12	13	14	15	16	17
γ_{max} (%)	9.98	14.98	11.24	16.23	8.32	11.65	13.32	18.31	14	20.95	12.48	15.33	12.89	12.48	15.13	9.98	14.98

As mentioned above, in hydrostatic forming technology, the thinnest area is the corner radius at the bottom of the product. In this area, there is a dangerous position with the largest thinning ratio. These values on each product are summarized in Table 6.

A mathematical model based on the theory of the orthogonal second-order design with 3 variables is represented by Eq. (7) [25].

$$Y = b_0 + \sum_{j=1}^3 b_j x_j + \sum_{i,j=1;i \neq j}^3 b_{ij} x_i x_j + \sum_{j=1}^3 b_{jj} x_j^2 \tag{7}$$

Where, b_j and b_{ij} are the coefficients of the regression function;

Testing of adequacy has been conducted with mathematical analysis according to F-distribution [25]. The condition $F_\alpha \leq F_t$ is satisfied as shown in Eq. (8):

$$F_\alpha = 2.14 < F_t = 19.41 \tag{8}$$

Where F_t is the tabulated value according to Fisher criterion, F_α is the adequacy according to Fisher criterion;

Test with regression coefficients R for mathematical equation obtained using the Eq. (9):

$$R = \sqrt{1 - \frac{\sum_{j=1}^N (Y_j^E - Y_j^R)^2}{\sum_{j=1}^N (Y_j^E - Y^*)^2}} = 0.9918 \tag{9}$$

$$Y^* = \frac{\sum_{j=1}^N Y_j^E}{N} \tag{10}$$

Where Y^* is the arithmetic mean of all experimental results as shown in Eq. (10), Y_j^E is the value of experimental results, Y_j^R is the calculation values of the obtained model;

The coefficient of determination R^2 is determined by the quality and reliability of the model as shown in Eq. (11):

$$R^2 = 0.9959 \tag{11}$$

The obtained results of the coefficient of determination R^2 indicate that 99.59% of the variability is attributed to the operation of the input variables (x_i). Final, decoded form of mathematical model for the largest thinning ratio γ_{max} is given in polynomial Eq. (12).

$$\gamma_{max} = -0.81 + 0.15 Q^* - 1.4 H^* + 2.11.H^*.S^* + 27.71.S^* - 45.37.S^{*2} \tag{12}$$

Comparing the values of experiments with the values obtained from mathematical model in the Eq. (12) is shown in Figure 7. It can be noticed that the difference between experimental results and calculated results from mathematical models is not significant. The largest error of experimental results and modelled results is 15.95 % and the average error is 5.7 %.

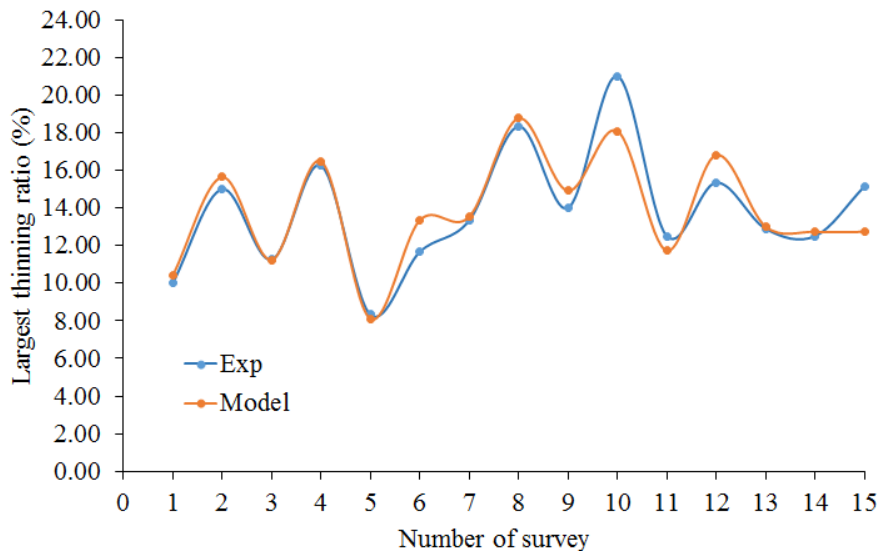


Figure 7. Comparison of modelled and experimental results

Evaluation the Effect of Each Variable on the Largest Thinning Ratio

The research has shown that the largest thinning ratio γ_{max} depends on x_2 (the relative depth of die) at the highest extent, and the depending extent decreases with respect to x_1 (the blank holder pressure) and x_3 (the relative thickness of workpiece) alternatively.

Using the Eq. (12) to assess the effect of each factor on the largest thinning ratio, it is necessary to consider the fixed values of each factor. Graphs are established from the Eq. (12) using Matlab, from which maximum and minimum value of γ_{max} can be figured out.

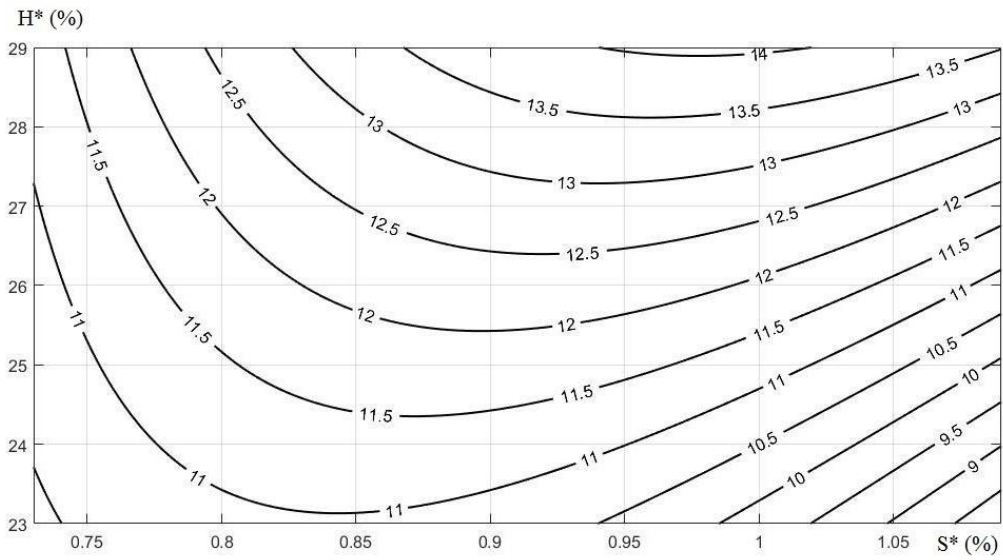


Figure 8. Dependence of γ_{\max} on H^* and S^* at $Q^* = 80$ bar

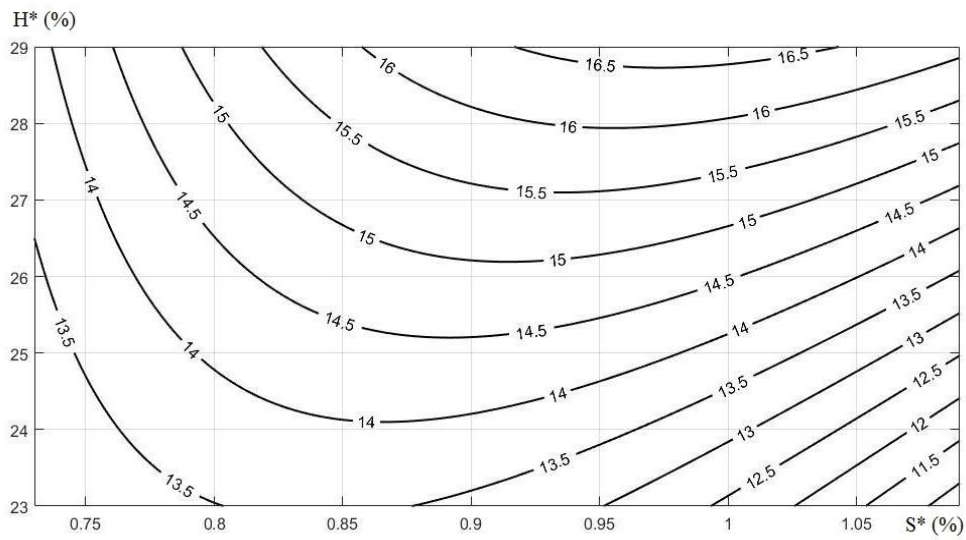


Figure 9. Dependence of γ_{\max} on H^* and S^* at $Q^* = 97.5$ bar

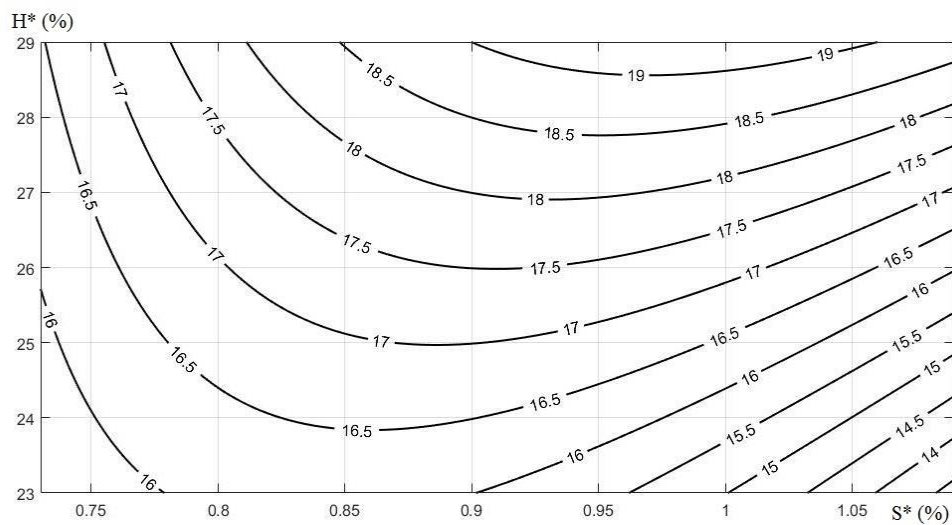


Figure 10. Dependence of γ_{\max} on H^* and S^* at $Q^* = 115$ bar

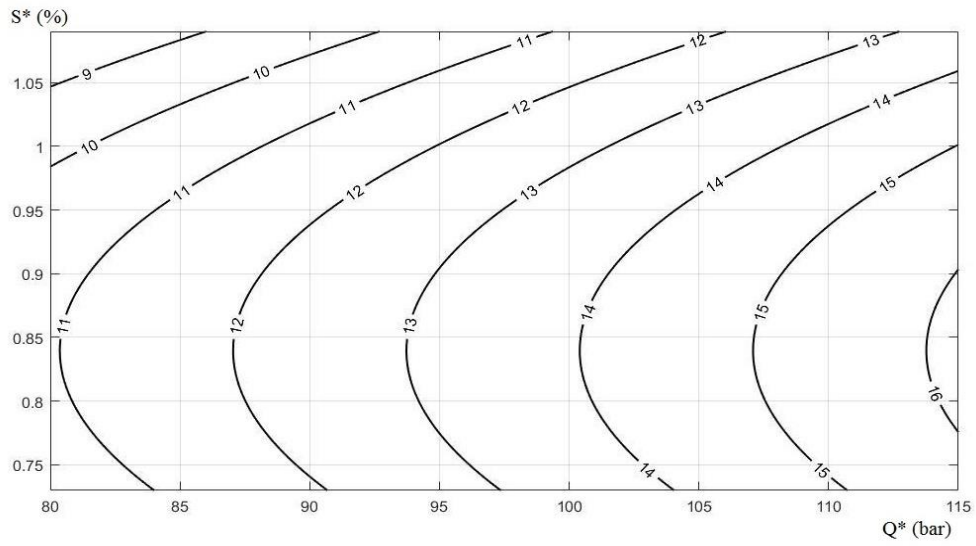


Figure 11. Dependence of γ_{\max} on S^* and Q^* at $H^* = 23\%$

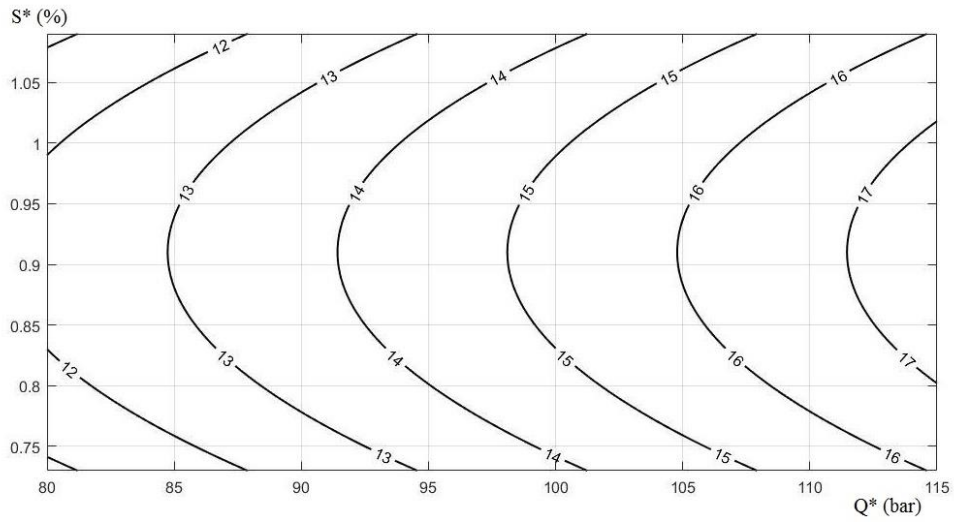


Figure 12. Dependence of γ_{\max} on S^* and Q^* at $H^* = 26\%$

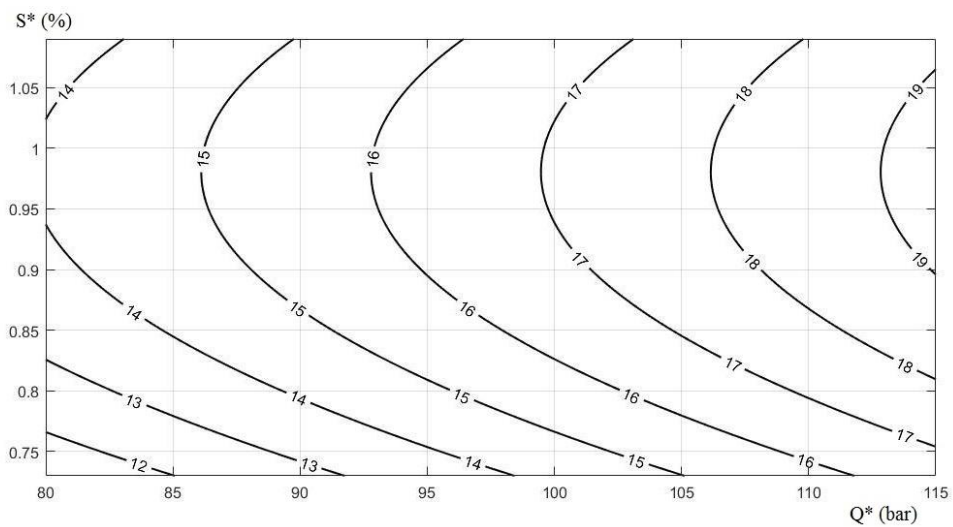


Figure 13. Dependence of γ_{\max} on S^* and Q^* at $H^* = 29\%$

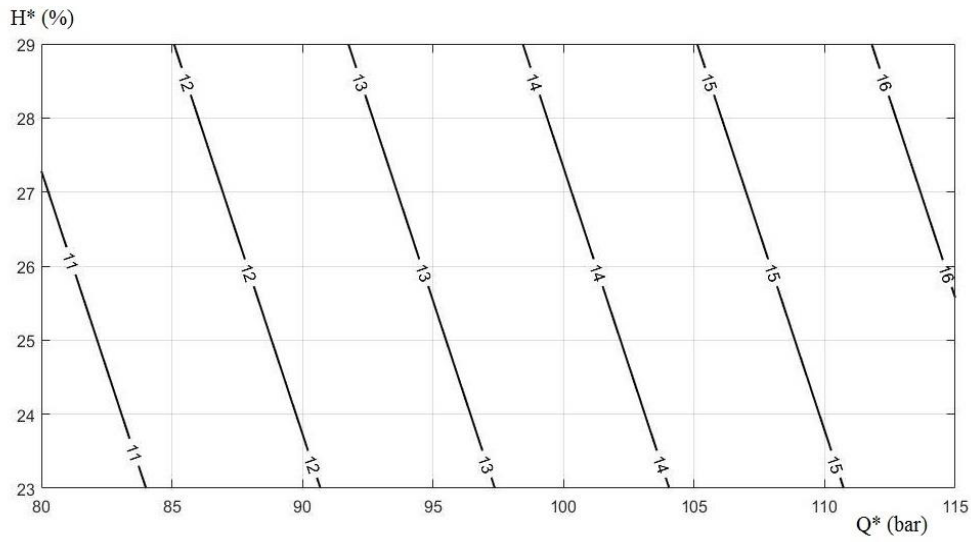


Figure 14. Dependence of γ_{\max} on H^* and Q^* at $S^* = 0.73\%$

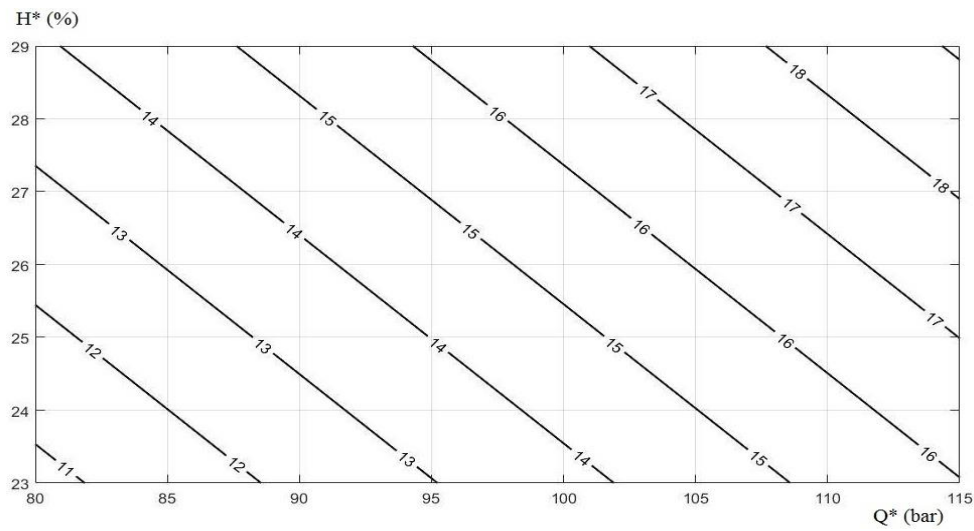


Figure 15. Dependence of γ_{\max} on H^* and Q^* at $S^* = 0.91\%$

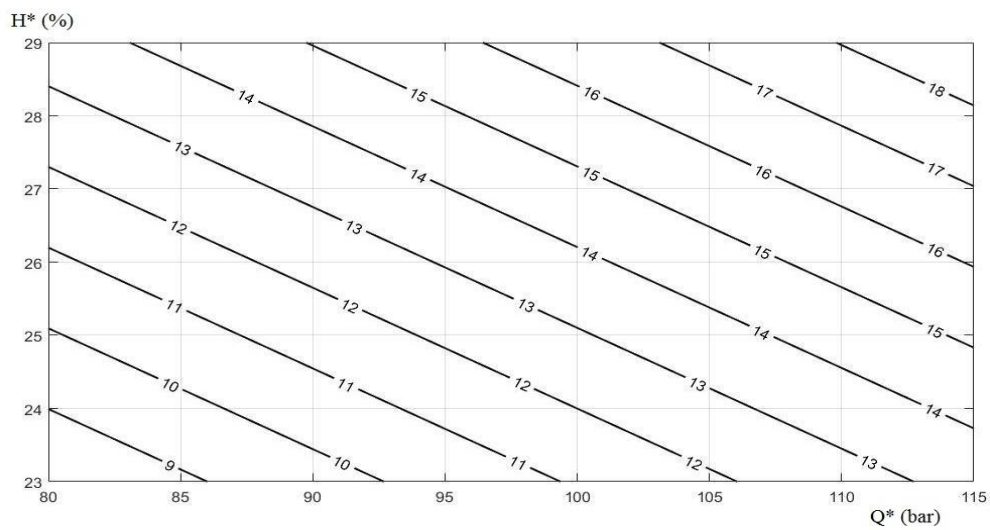


Figure 16. Dependence of γ_{\max} on H^* and Q^* at $S^* = 1.09\%$

The Eq. (12) and Figures (8-16) show the influence of the surveyed parameters including (Q^* , H^* , S^*) on the values of γ_{\max} . It can be seen that the dependence of γ_{\max} on S^* is more complicated than the other variables. There is the best value of S^* , where γ_{\max} reaches the minimum value shown in Figures (8-13).

When the relative depth of the die H^* increases, the free-bulging phase takes longer, so under the effect of forming pressure, the product becomes thinner.

When the blank holder pressure Q^* increases, it is more difficult to pull the workpiece into the cavity of die, so the formed product becomes thinner. Moreover, in the case of large values of Q^* , forming pressure also reaches high values. This forming pressure affects the workpiece, making the workpiece better deformed, especially at the corners of the die's bottom. Under the effect of large forming pressure and blank holder pressure, the workpiece will be more deformed, so the thinning increases.

The graphs in Figures (8-13) also show the effect of the relative thickness of workpiece S^* on the largest thinning ratio. Its impact on thinning variation is more complicated than the other two independent variables. It can be seen that in the cases under consideration, there always exists the most appropriate S^* value to achieve the smallest value of γ_{\max} .

Thus, based on the empirical the Eq. (12), it is possible to determine the appropriate values of input variables to achieve the smallest thinning ratio. In this study, in order to the smallest thinning level, the optimal input parameters (Q^* , H^* , S^*) are 80 bar, 23% and 1.09%, respectively.

Verification of the Applicability of the Equation

In order to verify the applicability of the Eq. (12), a cylindrical product with diameter of 60 mm and a height of 15 mm is investigated. The product is formed from a workpiece with an initial thickness of 0.8 mm and a diameter of 100 mm. As such, the relative height of the product H^* is 25% and the relative thickness of the product S^* is 0.8 %.

The surveyed values of blank holder pressure Q^* are 80, 90, 100, 110, 115 bar respectively. The values of the largest thinning ratio γ_{\max} are determined by the Eq. (12), and by experiment as shown in Figure 17. The biggest error between the experimental values and the modelled values is 5.3 % which is within the permissible error limit of the equation. Therefore, the Eq. (12) can be used to predict the largest thinning ratio of a product within its range of the research.

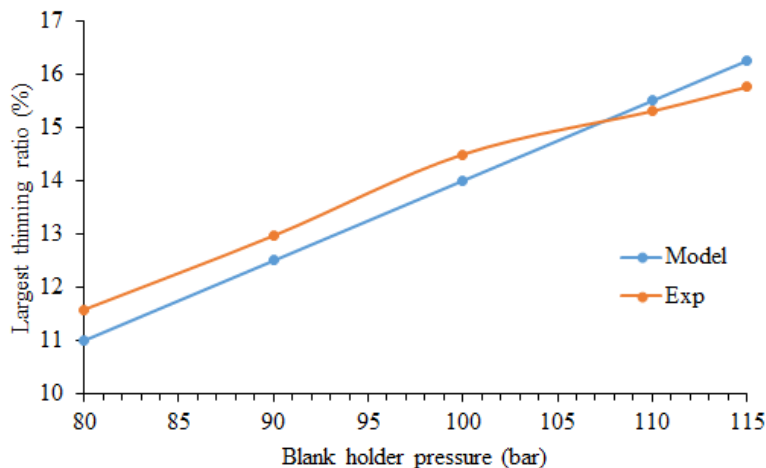


Figure 17. Comparison of modelled and experimental results for other products

CONCLUSIONS

The research results have made a considerable contribution to the number of research as well as the development in the field of hydrostatic forming. The experimental research indicates the thickness distribution of the product and the relationship between the largest thinning ratio and the input parameters.

Thickness distribution is proven to be non-uniform. In hydrostatic forming, thickening occurs on one part or the whole of the flange while thinning occurs in the rest of the product. For the product of this study, the region of radius at the bottom is the thinnest. This is a dangerous area that needs attention to avoid damage. The mathematical model of largest thinning ratio shows that this parameter depends the most on the relative height of die, then in turn on the blank holder pressure and the relative thickness of workpiece. A series of mathematical verifications regarding to the homogeneity of results, reliability and completeness testing of mathematical model have been carried out to confirm highly reliable mathematical model. Comparing experimental results and calculated results from the model, the deviations of the results are acceptable. Considering another product with different dimension in the study area, the difference in the maximum thinning ratio from the equation and experiment is also small.

The mathematical model for thinning variation is necessary because it helps to evaluate the thinning that occurs on the product. Therefore, it is possible to know if the product meets the requirements. From there, manufacturers can choose the appropriate parameters to shape the product.

REFERENCES

- [1] Ng, C. H., Lai, C. F., M. Yahaya, S. N., Shamsudin, S., S. Ahmad, S. N. A., Sharrifuddin, F., "Effect of initial blank temperature in hot press forming towards 22MnB5 springback failure," *J. Mech. Eng. Sci.*, vol. 13, no. 2, pp. 5137 - 5149., 2019, <https://doi.org/10.15282/jmes.13.2.2019.25.0422>.
- [2] Özek, C. and M. Bal, "The effect of die/blank holder and punch radiuses on limit drawing ratio in angular deep-drawing dies," *Int. J. Adv. Manuf. Technol.*, vol. 40, pp. 1077–1083, 2009, <https://doi.org/10.1007/s00170-008-1435-3>.
- [3] Abedrabbo, N., M. A.Zampaloni, and FarhangPourboghtr, "Wrinkling control in aluminum sheet hydroforming," *Int. J. Mech. Sci.*, vol. 47, no. 3, pp. 333-358, 2005, <https://doi.org/10.1016/j.ijmecsci.2005.02.003>.
- [4] R. Srinivasan, D. V., P. Padmanabhan, "Prediction of bend force and bend angle in air bending of electrogalvanized steel using response surface methodology," *J. Manuf. Sci. Technol.*, vol. 27, no. 7, pp. 2093-2105, 2013, DOI 10.1007/s12206-013-0528-6.
- [5] Swagatika Mohanty, S. P. R., Yendluri Venkata Daseswara Rao, "Influence of process parameters on surface roughness and forming time of Al-1100 sheet in incremental sheet metal forming," *J. Mech. Eng. Sci.*, vol. 13, no. 2, pp. 4911-4927, 2019, <https://doi.org/10.15282/jmes.13.2.2019.11.0408>.
- [6] M. Mianroodi, G. A., S. Touchal, "Experimental and numerical FEM-based determinations of forming limit diagrams of St14 mild steel based on Marciniak-Kuczynski model," *J. Mech. Eng. Sci.*, vol. 13, no. 4, pp. 5818-5831, 2019, <https://doi.org/10.15282/jmes.13.4.2019.08.0464>.
- [7] M., T., "Hydroforming applications in automotive: a review," *Int. J. Mater. Form.*, vol. 3, no. S1, pp. 307-310, 2010, 10.1007/s12289-010-0768-2.
- [8] Zahedi, S. A., H.Goodarzian, M.Okazi, and M. Bakhshi-Jooybari, "Investigation of conventional deep drawing and hydroforming deep drawing via experimental and finite element simulation," *Indian J.Sci.Technol.*, vol. 3, no. 9, pp. 1009-1013, 2010, 10.17485/ijst/2010/v3i9/29878
- [9] Kocanda, A. and H. Sadlowska, "Automotive component development by means of hydroforming," *Arch. Civ. Mech. Eng.*, vol. 8, no. 3, 2008, 10.1016/S1644-9665(12)60163-0.
- [10] Oh, S.-I., B.-H. Jeon, H.-Y. Kim, and J.-B. Yang, "Applications of hydroforming processes to automobile parts," *J. Mater. Process. Tech.*, vol. 174, no. 1, pp. 42-55, 2006, 10.1016/j.jmatprotec.2004.12.013.
- [11] Bell, C., J. Corney, N. Zuelli, and D. Savings, "A state of the art review of hydroforming technology," *Int. J. Mater. Form.*, 2019, 10.1007/s12289-019-01507-1.
- [12] Lang, L. H. *et al.*, "Hydroforming highlights: sheet hydroforming and tube hydroforming," *J. Mater. Process. Technol.*, vol. 151, no. 1-3, pp. 165-177, 2004, 10.1016/j.jmatprotec.2004.04.032.
- [13] S.H.Zhang, Z.R.Wang, Y.Xu, Z.T.Wang, and L.X.Zhou, "Recent developments in sheet hydroforming technology," *J. Mater. Process. Technol.*, vol. 151, no. 1-3, pp. 237-241, 2004, <https://doi.org/10.1016/j.jmatprotec.2004.04.054>.
- [14] Maki, T. and J. Cheng, "Sheet Hydroforming and Other New Potential Forming Technologies," *IOP Conference Series: Materials Science and Engineering*, vol. 418, p. 012117, 2018, 10.1088/1757-899x/418/1/012117.
- [15] Vasile, R., "Designing a Die for Hydroforming," *ACTA Universitatis Cibiniensis*, vol. 68, no. 1, pp. 7-11, 2016, 10.1515/aucts-2016-0002.
- [16] Bell, C. *et al.*, "Enabling sheet hydroforming to produce smaller radii on aerospace nickel alloys," *Int. J. Mater. Form.*, vol. 12, no. 5, pp. 761-776, 2018, 10.1007/s12289-018-1446-z.
- [17] Mevlüt Türköz, E. Ö., H. Selçuk Halkacı, Murat Dilmeç, "Manufacturing of Cups by Warm Hydroforming Process," presented at the 2nd International Conference on Science, Ecology and Technology-2016, 2016. Available: https://www.researchgate.net/publication/312198032_Manufacturing_of_Cups_by_Warm_Hydroforming_Process
- [18] Olayinka, A., W. J. Emblom, T. C. Pasacreta, and S. W. Wagner, "The Effect of Hydraulic Bulge Process on the Surface Topography of Annealed AISI 304 Stainless Steel," *Procedia Manufacturing*, vol. 10, pp. 243-252, 2017, 10.1016/j.promfg.2017.07.052.
- [19] Marandi, F. A., A. H. Jabbari, M. Sedighi, and R. Hashemi, "An Experimental, Analytical, and Numerical Investigation of Hydraulic Bulge Test in Two-Layer Al-Cu Sheets," *J. Manuf. Sci. E.*, vol. 139, no. 3, p. 10, 2017, 10.1115/1.4034717.
- [20] Colin Bell, D. S. T., Prof Jonathan Corney, David Savings, Nicola Zuelli, "Research directions in hydroforming technology," in *AIP Conference Proceedings* 2016, vol. 1769, no. 1.
- [21] Modi, B. and D. R. Kumar, "Development of a hydroforming setup for deep drawing of square cups with variable blank holding force technique," *Int. J. Adv. Manuf. Technol.*, vol. 66, no. 5-8, pp. 1159-1169, 2012, 10.1007/s00170-012-4397-4.
- [22] Taye, F. F. and K. D. Ravi, "Enhancement of drawability of cryorolled AA5083 alloy sheets by hydroforming," *J. Mater. Res. Technol.*, vol. 8, no. 1, pp. 411-423, 2019, 10.1016/j.jmrt.2018.02.012.
- [23] Zhang, S.-H., L.-X. Zhou, Z.-T. Wang, and Y. Xu, "Technology of sheet hydroforming with a movable female die," *Int. J. Mach. Tools Manuf.*, vol. 43, no. 8, pp. 781-785, 2003, 10.1016/s0890-6955(03)00057-9.

- [24] TakeoNakagawa, KazubikoNakamura, and HiroyukiAmino, "Various applications of hydraulic counter-pressure deep drawing," *J. Mater. Process. Technol.*, vol. 71, no. 1, pp. 160-167, 1997, [https://doi.org/10.1016/S0924-0136\(97\)00163-5](https://doi.org/10.1016/S0924-0136(97)00163-5).
- [25] Dougherty, C., *Introduction to Econometrics*, 2nd ed. OUP Oxford, 2002.